

Figure 1.2.1: Graphical representation of process by which a fermion, bouncing inelastically off the surface, sets it into vibration. Particles are represented by an arrowed line pointing upwards which is also the direction of time, while the vibration is represented by a wavy line. In the cartoon to the right, the black dot represents a nucleon moving in a spherical mean field of which it excites an octupole vibration after bouncing inelastically off the surface.

Random Phase Approximation (RPA) making use of the same interaction⁵ (Fig. 1.2.3), extending the selfconsistency to fluctuations $\delta\rho$ of the density and δU of the mean field, that is,

$$\delta U(r) = \int d\mathbf{r}' \delta\rho(\mathbf{r}') v(|\mathbf{r} - \mathbf{r}'|) \quad (1.2.7)$$

Making use of the solution to this relation one obtains the transition density $\delta\rho$. The matrix elements $\langle n_\lambda | v_i | \delta\rho | v_k \rangle$ provide the particle-vibration coupling strength to work out the variety of coupling processes between single-particle and collective motion (Fig. 1.2.1). That is, the matrix element of the PVC Hamiltonian H_c . Diagonalizing ~~X~~

$$H = H_{HF} + H_{RPA} + H_c + v, \quad (1.2.8)$$

by applying in the basis of single-particle and collective modes, that is solutions of H_{HF} and of H_{RPA} respectively, the NFT rules (see next chapter) one obtains an exact solution of the total Hamiltonian. Concerning the rules of NFT (Sect. 2.7), they codify the way in which H_c (three-point vertices) and v (four-point vertices) are to be ~~bubble~~^{graphical} (ring).

⁵ The sum of the so called ladder diagrams (see Fig. 1.2.3) are taken into account to infinite order in RPA. This is the reason why bubble contributions in the diagonalization of Eq. (1.2.8) are not allowed in NFT, being already contained in the basis states (see next chapter, Sect. 2.7).

*) @-@
P. (22) a
handwritten to order $1/S_2$ of the Feynman diagrams
calculated. The quantity S_2 is
the effective degeneracy in which
the nucleonic excitations are
allowed to correlate through v

(d) Footnote call before Eq. (1,2,8)

* According to renormalized NFT, v is the NN-interaction which eventually combined with a \hbar -mass, is used to calculate the bare single-particle states (HF-approximation), ~~the~~ collective vibration (RPA) and particle-vibration coupling vertices so that once the corresponding renormalization (dressing) ^(including also four-point vertices, i.e. v) diagrams are worked to the order of $1/\hbar^2$ required (eventually infinite order if needed), reproduce the experimental findings. It is of notice that if one is interested in the collective vibrations, only to dress the single-particle degrees of freedom, one can take them from experiment. In other words, determine the Λ -values by making use of the ^{of the experimental} dynamical deformation parameters $\beta_\lambda = \sqrt{\frac{\hbar\omega_\lambda}{2C_\lambda}} \frac{1}{\sqrt{2\lambda+1}}$ and energies $\hbar\omega_\lambda$ (Broglia et al (2016)), in conjunction to the expression of the RPA amplitudes X and Y and dispersion relation collected in the caption to Fig. 1,2,3.

to p. 22 (d)

* R.A.Broglia et al Phys. Scr. (2016).

(a) - (b)

be treated to all orders of perturbation theory. Also which processes (diagrams) are not allowed because they will imply overcounting of correlations already included in the basis states⁶.

from
p.
(23) a
hand
written

Because of quantal zero point fluctuations, a nucleon propagating in the nuclear medium moves through a cloud of bosonic virtual excitations to which it couples becoming dressed and acquiring effective mass, charge, etc. (Fig. 1.2.4; see also App. 5.A and 5.H). Vice versa, vibrational modes can become renormalized through the coupling to dressed nucleons which, in intermediate virtual states, can exchange the vibrations which produce their clothing, with the second fermion (hole state). Such a process leads to a renormalization of the PVC vertex⁷ (Fig. 1.2.5), as well as of the bare NN -interaction, in particular 1S_0 component (bare pairing interaction)⁸.

The analytic procedures equivalent to the diagrammatic ones to obtain the HF (Fig. 1.2.2) and RPA (Fig. 1.2.3) solutions associated with the bare NN -interaction v is provided by the relations (1.1.16) and (1.1.15) respectively, replacing the corresponding Hamiltonians by $(T + v)$, where T is the kinetic energy operator. The phonon operator associated with surface vibrations is defined as,

$$\Gamma_\alpha^\dagger = \sum_{ki} X_{ki}^\alpha \Gamma_{ki}^\dagger + Y_{ki}^\alpha \Gamma_{ki}, \quad (1.2.9)$$

the normalization condition being,

$$[\Gamma_\alpha, \Gamma_\alpha^\dagger] = \sum_{ki} (X_{ki}^{\alpha 2} - Y_{ki}^{\alpha 2}) = 1. \quad (1.2.10)$$

The operator $\Gamma_{ki}^\dagger = a_k^\dagger a_i (\epsilon_k > \epsilon_F, \epsilon_i \leq \epsilon_F)$ creates a particle-hole excitation acting on the HF vacuum state $|0\rangle_F$. It is assumed that

$$[\Gamma_{ki}, \Gamma_{k'i'}^\dagger] = \delta(k, k')\delta(i, i'). \quad (1.2.11)$$

Within this context, RPA is a harmonic, quasi-boson approximation.

From being antithetic views of the nuclear structure, a proper analysis of the experimental data testifies to the fact that the collective and the independent particle pictures of the nuclear structure require and support each other (Bohr, A. and Mottelson (1975)). To obtain a quantitative description of nucleon motion and nuclear phonons (vibrations), one needs a proper description of the k - and ω -dependent “dielectric” function of the nuclear medium, in a similar way in which a proper

⁶A simple, although not directly related but only in a general way, example is provided by Eq. (2A-31) of Bohr and Mottelson (1969) i.e. $G = \frac{1}{4} \sum_{v_1 v_2 v_3 v_4} \langle v_3 v_4 | G | v_1 v_2 \rangle_a a^\dagger(v_4) a^\dagger(v_3) a(v_1) a(v_2) = \frac{1}{2} \sum_{v_1 v_2 v_3 v_4} \langle v_3 v_4 | G | v_1 v_2 \rangle_a a^\dagger(v_4) a^\dagger(v_3) a(v_1) a(v_2)$ where $\langle \cdot \rangle_a$ is the antisymmetric matrix element.

Bertsch et al. (1983); Barranco et al. (2004) and refs. therein. It is to be noted that in the case in which the renormalized vibrational modes, i.e. the initial and final wavy lines in Fig. 1.2.5 have angular momentum and parity $\lambda^\pi = 0^+$, and one uses a model in which there is symmetry between the particle and the hole subspaces, the four diagrams sum to zero, because of particle (gauge) conservation.

⁸See e.g. Brink, D. and Broglia (2005) Ch. 10 and references therein.

to give rise to the collective mode,
 $\sqrt{\omega}$ being the small parameter
of the NFT diagrams (see Sect. 2.7.2
as well as 7.6.2)

* footnote

(w) to p. 23

(23)_a

Before proceeding let us make a simple estimate of the coupling strength κ , making use of a schematic separable interaction

$$V = -\kappa \hat{F} \hat{F}^\dagger \quad (1.2.9)$$

and of an expansion of the nuclear density $\rho(r, R)$ similar to (1.2.2), that is,

$$\delta P(\vec{r}) = -R_0 \frac{\partial P(r)}{\partial r} Y_{\lambda\mu}^*(\hat{r}). \quad (1.2.10)$$

With the help of the dynamical self-consistent relation (1.2.7) one obtains*

$$\kappa = \int r^2 dr R_0 \frac{\partial P(r)}{\partial r} R_0 \frac{\partial U(r)}{\partial r}. \quad (1.2.11)$$

For attractive fields, both V and κ are negative.

(w)

to p. 23

*) Bohr and Mottebo (1975)

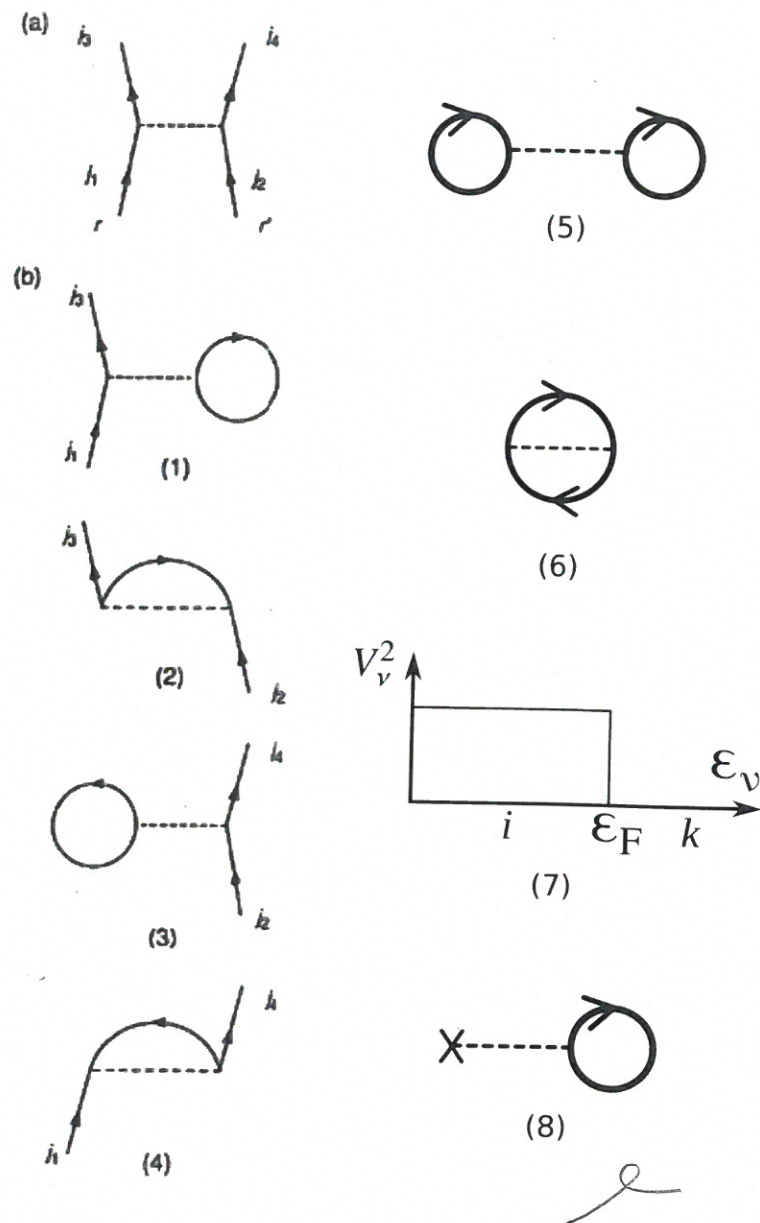


Figure 1.2.2: (a) Scattering of two nucleons through the ~~bare~~ NN -interaction; (b) (1) and (3): Contributions to the (direct) Hartree potential; (2) and (4): contributions to the (exchange) Fock potential. In (5) and (6) the ground state correlations associated with the Hartree- and the Fock-terms are displayed. (7) States $|i\rangle$ ($\epsilon_i \leq \epsilon_F$) are occupied with probability $V_i^2 = 1$. States $|k\rangle$ ($\epsilon_k > \epsilon_F$) are empty $V_k^2 = 1 - U_k^2$. (8) Nuclear density, the density operator being represented by a cross followed by a dashed horizontal line. (After Brink, D. and Broglia (2005)).

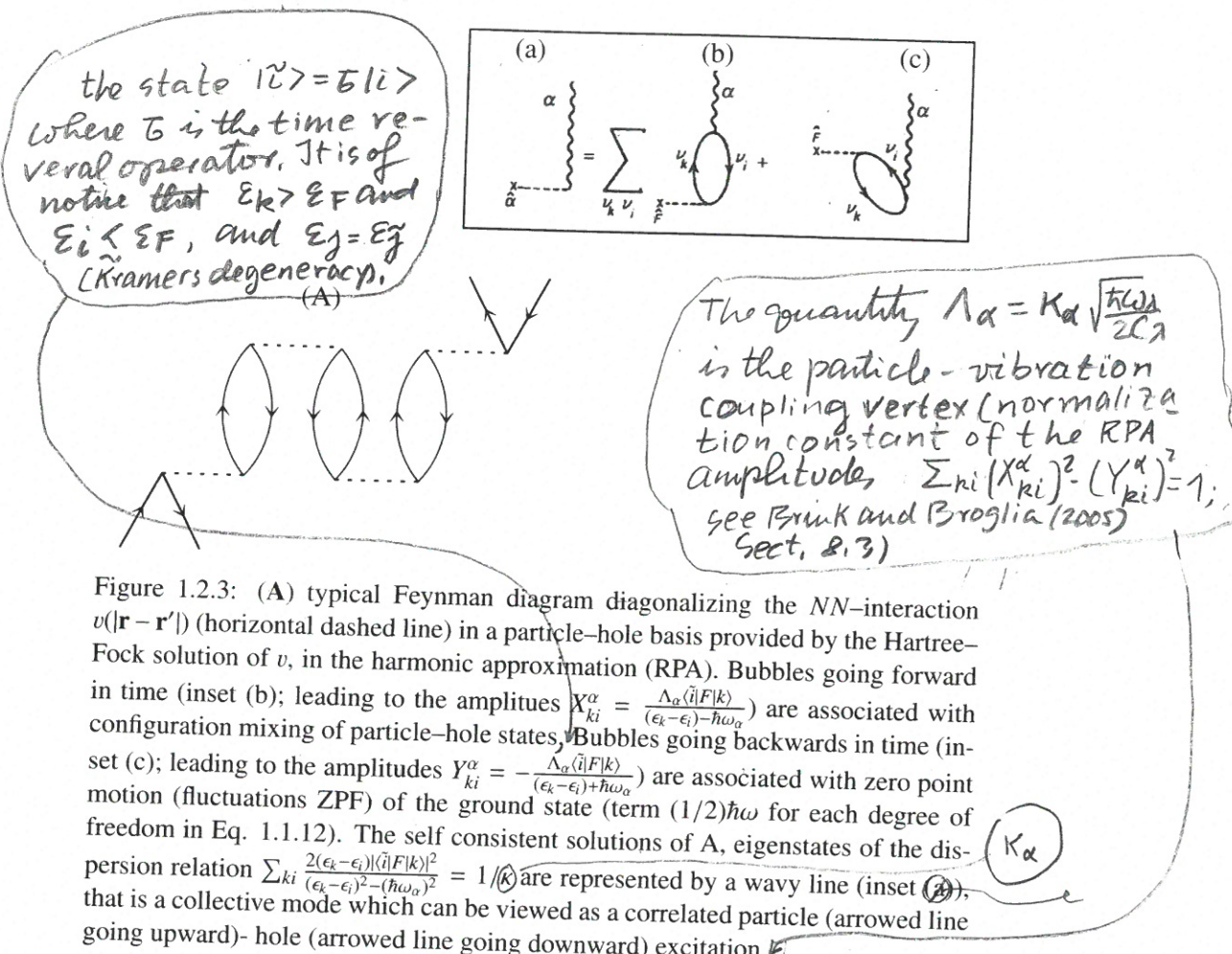
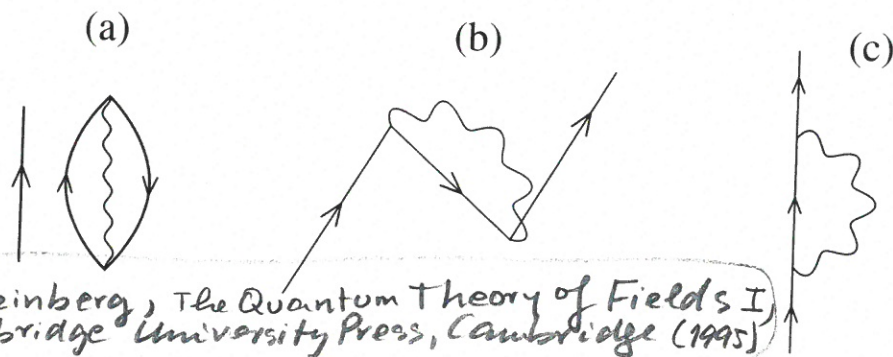


Figure 1.2.3: (A) typical Feynman diagram diagonalizing the NN -interaction $v(|\mathbf{r} - \mathbf{r}'|)$ (horizontal dashed line) in a particle-hole basis provided by the Hartree-Fock solution of v , in the harmonic approximation (RPA). Bubbles going forward in time (inset (b); leading to the amplitudes $X_{ki}^\alpha = \frac{\Lambda_\alpha \langle i|F|k \rangle}{(\epsilon_k - \epsilon_i) - \hbar\omega_\alpha}$) are associated with configuration mixing of particle-hole states. Bubbles going backwards in time (inset (c); leading to the amplitudes $Y_{ki}^\alpha = -\frac{\Lambda_\alpha \langle i|F|k \rangle}{(\epsilon_k - \epsilon_i) + \hbar\omega_\alpha}$) are associated with zero point motion (fluctuations ZPF) of the ground state (term $(1/2)\hbar\omega$ for each degree of freedom in Eq. 1.1.12). The self consistent solutions of A , eigenstates of the dispersion relation $\sum_{ki} \frac{2(\epsilon_k - \epsilon_i) \langle i|F|k \rangle^2}{(\epsilon_k - \epsilon_i)^2 - (\hbar\omega_\alpha)^2} = 1/\hbar$ are represented by a wavy line (inset (A)), that is a collective mode which can be viewed as a correlated particle (arrowed line going upward)- hole (arrowed line going downward) excitation.



S. Weinberg, The Quantum Theory of Fields I,
Cambridge University Press, Cambridge (1995)

Figure 1.2.4: (a) a nucleon (single arrowed line pointing upward) moving in presence of the zero point fluctuation of the nuclear ground state associated with a collective surface vibration; (b) Pauli principle leads to a dressing process of the nucleon; (c) time ordering gives rise to the second possible lowest order clothing process (time assumed to run upwards). The above are phenomena closely related with the Lamb shift of Quantum Electrodynamics (see e.g. Weinberg (1995) Sect. 14.3)

description of the reaction processes used as probes of the nuclear structure requires the use of the optical potential (continuum "dielectric" function). The NFT solution of (1.2.8) provides all the elements to calculate the structure properties of nuclei, and also the optical potential needed to describe nucleon-nucleus as well as the nucleus-nucleus scattering and reaction processes. It furthermore shows that both single-particle and vibrational elementary modes of excitation emerge from the same properties of the NN -interaction, the main task being that of relating these modes with the observables. Namely with the absolute differential cross sections, in keeping with the central role played by the quantal many-body renormalization processes and associated emergent properties. Renormalization which acts on par on the radial dependence of the wavefunctions (formfactors) and on the single-particle content of the orbitals involved in the reaction process under discussion (see e.g. Sect. 7.2). In other words, structure ad reactions are to be treated on equal footing⁹. *(mixing with collective states)*

The development of experimental techniques and associated hardware has allowed for the identification of a rich variety of elementary modes of excitation aside from collective surface vibrations and of independent particle motion: quadrupole and octupole rotational bands, giant resonance of varied multipolarity and isospin, as well as pairing vibrations and rotation, together with giant pairing vibrations of transfer quantum number $\beta = \pm 2$. Modes which can be specifically excited in inelastic and Coulomb excitation processes (see App. 2.A), and one- and two-particle transfer reactions (Ch. 6).

$$\beta = \pm 2.$$

1.3 Pairing vibrations

Let us introduce this new type of elementary mode of excitation by making a parallel with quadrupole surface vibrations within the framework of RPA, namely

$$[(H_{sp} + H_i), \Gamma_{k'i'}^\dagger] = \hbar\omega_\alpha \Gamma_{k'i'}^\dagger, \quad (1.3.1)$$

where for simplicity we use, instead of v , a quadrupole-quadrupole separable interaction ($i = QQ$) defined as

$$H_{QQ} = -\kappa Q^\dagger Q \quad (1.3.2)$$

with

$$Q^\dagger = \sum_{ki} \langle k | r^2 Y_{2\mu} | i \rangle a_k^\dagger a_i, \quad (1.3.3)$$

while H_{sp} and Γ_α^\dagger are defined in (1.1.13) and (1.2.9) supplemented by (1.2.10).

⁹ Within this context, and referring to one-particle transfer reactions for concreteness, the prescription of using the ratio of the absolute experimental cross section and the theoretical one – calculated in the Distorted Wave Born Approximation (DWBA) making use of Saxon-Woods single-particle wavefunctions as formfactors – to extract the single-particle content of the orbital under study (see e.g. Schiffer, J. P. et al. (2012)), may not be appropriate.

replace by
 ① - ④ p.
 27a
 handwritten

④ to p.27'

The NFT solutions of (1,2,8) provide all the elements to calculate the structure properties of nuclei, and also the optical potential needed to describe nucleon-nucleus as well as nucleus-nucleus elastic scattering and reaction processes.

Furthermore, the NFT solutions of (1,2,8) show that both single-particle (fermionic) and collective (bosonic) elementary modes of excitation emerge from the same properties of the NN-interaction. For example, a bunching of levels of the same or opposite parity just below and above the Fermi energy, imply low-lying quadrupole (e.g. $^{50}_{\Lambda}\text{Sn}$ -isotopes), or dipole ($^{11}_3\text{Li}_8$) or octupole ($^{208}_{82}\text{Pb}_{126}$) collective vibrational modes. And, as a bonus, one has the building blocks to build the nuclear spectrum, and bring quantitative simplicity into the experimental findings. Within this connection, the NFT solutions of (1,2,8) indicate the minimum set of experimental probes needed to have a "complete" picture of the nuclear structure associated with a given energy region. This is a consequence of the central role played by the quantum many-body renormalization process which interweave the variety of elementary modes of excitation. ④

to p.27

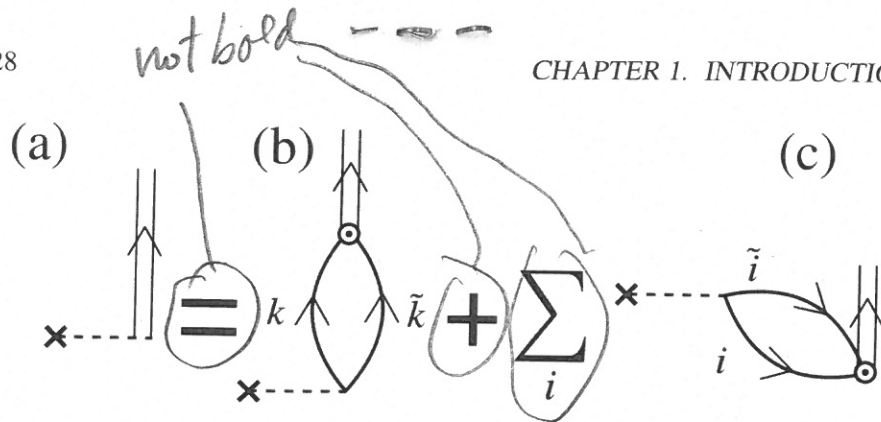


Figure 1.3.1: Graphical representation of the RPA dispersion relation describing the pair addition pairing vibrational mode, represented by a double arrowed line. Making use of the unitary transformation (1.3.6), a cross followed by a dashed horizontal line stands for: (a) the collective operator Γ_α^\dagger , (b) the operator Γ_k^\dagger creating a pair of nucleons moving in time reversal states associated with ground state correlations (k, \tilde{k}) above the Fermi energy ($\epsilon_k > \epsilon_F$); (c) The operator Γ_i^\dagger filling a pair of time reversal holes associated with ground state correlations ($\epsilon_i \leq \epsilon_F$).

reversed *(v, v̄)* *above (odd - even staggering)*

In connection with the pairing energy mentioned in relation with the inset to Fig. 1.1.1, it is a consequence of correlation of pairs of like nucleons moving in time reversal states! A similar phenomenon to that found in metals at low temperatures and giving rise to superconductivity. The pairing interaction ($i = p$) can be written, within the approximation (1.3.2) used in the case of the quadrupole-quadrupole force, as

$$(-G P^\dagger P) \rightarrow G \quad H_P = -P^\dagger P, \quad (1.3.4)$$

where

$$P^\dagger = \sum_{\nu>0} a_\nu^\dagger a_{\bar{\nu}}^\dagger. \quad (1.3.5)$$

and G is a pairing coupling constant.

Consequently, in this case the concept of independent particle field \hat{Q} (see also (1.2.4)) associated with particle-hole (ph) excitations and carrying transfer quantum number $\beta = 0$ has to be generalized to include fields describing independent pair motion, in which case $\alpha \equiv (\beta = +2, J^\pi = 0^+)$

$$\Gamma_\alpha^\dagger = \sum_k X_{kk}^\alpha \Gamma_k^\dagger + \sum_i Y_{ii}^\alpha \Gamma_i^\dagger \quad (1.3.6)$$

with

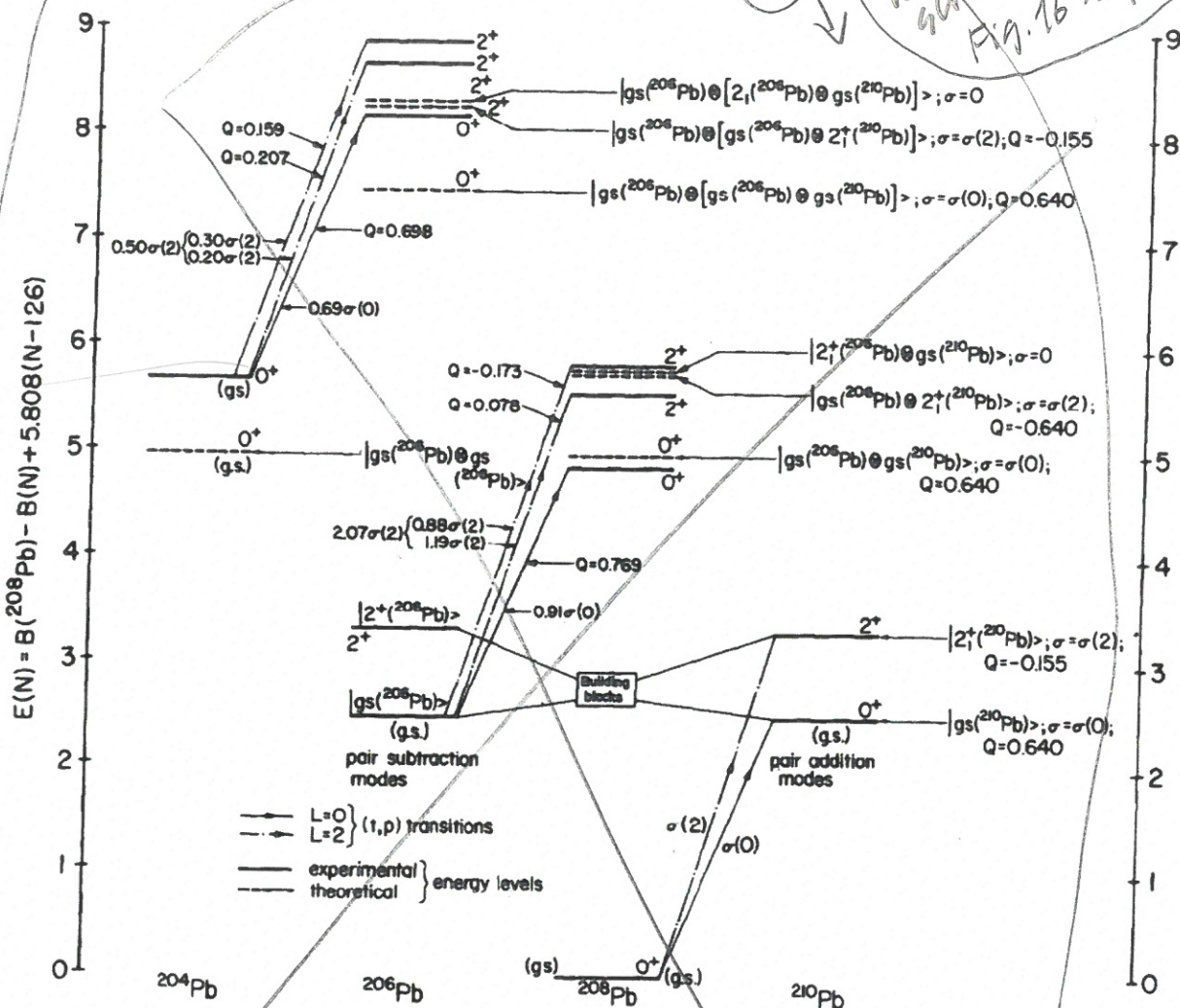
$$\Gamma_k^\dagger = a_k^\dagger a_{\bar{k}}^\dagger \quad (\epsilon_k > \epsilon_F), \quad \Gamma_i^\dagger = a_i^\dagger a_{\bar{i}}^\dagger \quad (\epsilon_i \leq \epsilon_F), \quad (1.3.7)$$

and

$$\sum_k X_{kk}^{\alpha 2} - \sum_i Y_{ii}^{\alpha 2} = 1, \quad (1.3.8)$$

of different multipolarity and (normal) parity, in particular 0^+ ,

1.3. PAIRING VIBRATIONS



Theoretical predictions of the pairing vibrational model for the $J^\pi = 0^+$ and 2^+ excited states of ^{208}Pb and ^{206}Pb expected to display the same Q -value, angular distribution and intensities in the $^{206}, ^{204}\text{Pb}$ (t, p) reactions as the ground state and first excited 2^+ state of ^{210}Pb in the ^{208}Pb (t, p) ^{210}Pb reaction.

These levels are depicted as dotted lines and their structure in terms of the pair addition and pair subtraction phonons (building blocks) are explicitly given.

The corresponding cross section and Q -values expected for each transition are also quoted for each state. The experimental energies (solid lines) and (t, p) cross sections are also given. In this case, the levels are joined by a continuous line ($L = 0$ transitions) or by a dotted line ($L = 2$ transitions) and the corresponding intensities in terms of the cross sections $\sigma(0) = \sigma(^{208}\text{Pb} \text{ (t, p)} ^{210}\text{Pb} \text{ (gs)})$ and $\sigma(2) = \sigma(^{208}\text{Pb} \text{ (t, p)} ^{210}\text{Pb} \text{ (2 \pm)})$ are given. Also quoted are the observed Q -values.

The experimental energy of the different ground states is given relative to the ^{208}Pb ground state and corrected by a linear function of the number of neutrons outside (or missing from) the $N = 126$ closed shell such that $E(^{206}\text{Pb (gs)}) = E(^{210}\text{Pb (gs)})$. The corresponding expression [6] is $E_{\text{exp}}(N, Z = 82) = B(^{208}\text{Pb}) - B(N, Z = 82) + 5.808(N-126)$, where $B(N, Z)$ is the binding energy of the nucleus $A = N + Z$. Note that $\hbar\omega(0) = E_{\text{theor}}(^{206}\text{Pb (gs)}) = E_{\text{theor}}(^{210}\text{Pb (gs)}) = E_{\text{exp}}(^{206}\text{Pb (gs)}) = E_{\text{exp}}(^{210}\text{Pb (gs)}) = 2.493$ MeV, that $E_{\text{theor}}(^{206}\text{Pb (2 \pm)}) = E_{\text{exp}}(^{206}\text{Pb (2 \pm)}) = 3.294$ MeV and $E_{\text{theor}}(^{210}\text{Pb (2 \pm)}) = E_{\text{exp}}(^{210}\text{Pb (2 \pm)}) = 3.288$ MeV. The theoretical energy of any other state, for example of the 2^+ state $|gs(^{206}\text{Pb}) \otimes 2(^{210}\text{Pb}; 2^+)$ of ^{206}Pb is equal to $2.493 + 3.294 + 2.493 = 8.280$ MeV (as measured from $^{208}\text{Pb (gs)}$).

Figure 1.3.2: (After Flynn, E. R. et al. (1972)).

Replace by
Fig. 5.5 p. 1D9
Brink + Braglia

for the pair addition ($(pp), \beta = +2$) mode, and a similar expression for the pair removal ($(hh), \beta = -2$) mode. In Fig. 1.3.1 the NFT graphical representation of the RPA equations for the pair addition mode is given. The state $\Gamma_a^\dagger(\beta = +2)|\tilde{0}\rangle$, where $|\tilde{0}\rangle$ is the correlated ground state of a closed shell nucleus, can be viewed as the nuclear embodiment of a Cooper pair found at the basis of the microscopic theory of superconductivity.

While surface vibrations are associated with the normal ($\beta = 0$) nuclear density, pairing vibrations are connected with the so called abnormal ($\beta = \pm 2$) nuclear density (density of Cooper pairs), both static and dynamic.

Similar to the quadrupole and octupole vibrational bands built out of n_α phonons of quantum numbers $\alpha \equiv (\beta = 0, \lambda^\pi = 2^+, 3^-)$ schematically shown in Fig. 1.1.4 and experimentally observed in inelastic and Coulomb excitation and associated γ -decay processes, pairing vibrational bands build of n_α phonons of quantum numbers $\alpha \equiv (\beta = \pm 2, \lambda^\pi = 0^+, 2^+)$ have been identified around closed shells in terms of two-nucleon transfer reactions throughout the mass table (see e.g. Fig. 1.3.2).

1.4 Spontaneous broken symmetry *(and to the degree of accuracy relevant in many-body problems also invariant under time-reversal, and time-reversal)*

Because empty space is homogeneous and isotropic, the nuclear Hamiltonian is translational and rotational invariant. It ~~also conserves particle number and is thus gauge invariant~~. According to quantum mechanics, the corresponding wavefunctions transform in an irreducible way under the corresponding groups of transformation. When the solution of the Hamiltonian does not have some of these symmetries, for example defines a privileged direction in space violating rotational invariance, one is confronted with the phenomenon of spontaneous broken symmetry. Strictly speaking, this can take place only for idealized systems that are infinitely large. But when one sees similar phenomena in atomic nuclei, although not so clear or regular, one recognizes that this system is after all a finite quantum many-body system (FQMBS).^{*}

1.4.1 Quadrupole deformations in 3D-space

A nuclear embodiment of the spontaneous symmetry breaking phenomenon is provided by a quadrupole deformed mean field. A situation one is confronted with, when the value of the lowest quadrupole frequency ω_2 of the RPA solution (1.1.15) tends to zero ($C_2 \rightarrow 0, D_2$ finite). A phenomenon resulting from the interplay of the interaction v (H_{QQ} in (1.3.2)), and of the nucleons outside closed shell, leading to tidal-like polarization of the spherical core.

Coordinate and linear momentum ((x, p_x) single-particle motion) as well as Euler angles and angular momentum ((φ, I_z) rotational in two-dimensional (2D)-space) are conjugate variables. Similarly, the gauge angle and the number of particles ((ϕ, N) rotation in gauge space), fulfill $[\phi, N] = i$. The operators $e^{-ip_x x}, e^{-i\varphi I_z}$ and $e^{-iN\phi}$ induce Galilean transformation and rotations in 2D- and in gauge space

*) P.W. Anderson (1972);

P W Anderson Basic Notions of Condensed Matter Physics (1997)

expression of the Nilsson potential includes, aside from the central term discussed above, a spin-orbit and a term proportional to the orbital angular momentum quantity squared, so as to make the shape of the oscillator to resemble more that of a Saxon-Woods potential. The resulting levels provide an overall account of the experimental findings, providing detailed evidence in terms of individual states of the interplay between the single-particle and the collective aspects of nuclear structure. An example of relevance for light nuclei (N and $Z < 20$) is given in Fig. 1.4.2.

The Nilsson intrinsic state (1.4.7) does not have a definite angular momentum but is rather a superposition of such states,

$$|N(\omega)\rangle_{\mathcal{K}'} = \sum \tilde{\mathcal{O}}_I^L |I\rangle. \quad (1.4.11)$$

Because there is no restoring force associated with different orientations of $|N(\omega)\rangle_{\mathcal{K}'}$, fluctuations in the Euler angle diverge in the right way to restore rotational invariance, leading to a rotational band whose members are

$$|IKM\rangle \sim \int d\omega \mathcal{D}_{MK}^I(\omega) |N(\omega)\rangle_{\mathcal{K}'}, \quad (1.4.12)$$

with energy

$$E_I = \frac{\hbar^2}{2I} I(I+1). \quad (1.4.13)$$

The quantum numbers I, M, K are the total angular momentum I , and its third component M and K along the laboratory (z) and intrinsic (z') frame references respectively. Rotational bands have been observed up to rather high angular momenta in terms of individual transitions. An example extending up to $I = 60\hbar$ is given in Fig. 1.4.3.

1.4.2 Deformation in gauge space

Let us now turn to the pairing Hamiltonian. In the case in which $\hbar\omega_{\beta=-2} = \hbar\omega_{\beta=2} = 0$, the system deforms, this time in gauge space. Calling $|BCS\rangle$ the mean field solution of the pairing Hamiltonian, leads to the finite expectation value

$$\alpha_0 = \langle BCS | P^\dagger | BCS \rangle, \quad (1.4.14)$$

of the pair creation operator P^\dagger , quantity which can be viewed as the order parameter of the new deformed phase of the system in gauge space. The total Hamiltonian can be written as

$$H = H_{MF} + H_{fluct}, \quad (1.4.15)$$

where

$$H_{MF} = H_{sp} - \Delta(P^\dagger + P) + \frac{\Delta^2}{G} \quad (1.4.16)$$